The L1 Cell Adhesion Molecule Is Essential for Topographic Mapping of Retinal Axons

Galina P. Demyanenko and Patricia F. Maness

Department of Biochemistry and Biophysics, University of North Carolina School of Medicine, Chapel Hill, North Carolina 27599-7260

The retinocollicular projection is a preferred axon guidance pathway for investigating molecular mechanisms of synaptic targeting in the mammalian CNS. Here we identify a previously unrecognized role of the L1 cell adhesion molecule in topographic mapping of retinal ganglion cell (RGC) axons to their targets in the mouse superior colliculus (SC). L1 was transiently expressed on RGC axons during axon growth and targeting. DiI labeling of retinal axons revealed that temporal axons of L1-minus mice bypassed correct target locations in the anterior SC, forming termination zones at incorrect posterior sites, which were often skewed along the mediolateral axis. During development of the retinotopic map L1-minus temporal axons extended across the anteroposterior axis of the SC like wild-type axons but failed to arborize at normal anterior target sites. L1-minus RGC axons exhibited normal crossing at the optic chiasm and fasciculation of the optic nerve. Results suggest that retinal axons require the function of L1 in addition to repellent EphA guidance receptors to achieve proper topographic mapping.

Key words: **L1; cell adhesion molecule; axon guidance; retinocollicular mapping; synaptic targeting; ephrin**

Introduction

The mapping of retinal ganglion cell (RGC) axons to their topographically matched targets in the superior colliculus (SC) is one of the best-defined axon guidance pathways in the mammalian CNS. In this pathway, RGC axons from graded positions within the retina are mapped to targets in the SC along both anteroposterior and dorsal-ventral axes to generate a spatially matched projection of visual images to the brain. The formation of connections between RGC axons and their targets along the anteroposterior axis of the SC depends on the interaction of complementary gradients of repellent ephrin-A ligands expressed in the SC and their receptors, the EphA tyrosine kinases expressed on retinal axons (for review, see Klein, 2001; Wilkinson, 2001). Studies with knock-out mice have indicated functions for ephrin-A2 and ephrin-A5 ligands and EphA receptors in targeting of temporal RGC axons to the anterior SC and nasal axons to the posterior SC (Frisen et al., 1998; Brown et al., 2000; Feldheim et al., 2000). Although temporal axons of ephrin-A2$^{-/-}$ephrin-A5$^{-/-}$ double mutant mice map more posteriorly than normal, and nasal axons map more anteriorly (Feldheim et al., 2000), topographic order in these mutants is not completely disrupted, suggesting that ephrin-As and EphA receptors are not sufficient to explain the retinotopic map.

The transmembrane adhesion molecule L1 (200 kDa) is an attractive candidate for regulating axon guidance in the retinocollicular pathway. L1 is expressed on growth cones and axons of premyelinated neurons in the developing brain and retina, where it is an important mediator of axon growth and fasciculation (Schachner, 1991). Through its six extracellular Ig-like and five fibronectin III domains, L1 participates in homophilic binding between opposing cells (Lemmon et al., 1989) and in heterophilic binding to TAG-1, β1-integrins, F11/contactin, neural cell adhesion molecule (NCAM), and proteoglycans (for review, see Schmid and Maness, 2001). Binding induces L1 clustering in the plasma membrane, which activates a MAP kinase signaling cascade through the intermediates Src, phospohinositide-3 kinase, Rac1, and p21-activated kinase, leading to neurite growth (Ignelzi et al., 1994; Schaefer et al., 1999; Schmid et al., 2000). L1 can functionally interact with certain cell surface receptors such as β1-integrins to potentiate neuronal migration (Mechtersheimer et al., 2001; Thelen et al., 2002) and with the semaphorin 3A receptor neuropilin-1 for repellent guidance of corticospinal axons (Castellani et al., 2000); thus L1 might cooperate with EphA receptors for retinotopic mapping. Potential interaction between L1 and Eph receptors is suggested by the phosphorylation of L1 by EphB2 in neuroblastoma cells (Zisch et al., 1997), although the consequences of this modification are not known.

L1 is the target for mutation in a human X-linked mental retardation syndrome characterized by cognitive impairment, spastic paraplegia, corpus callosum dysgenesis, and hydrocephalus (Kenwrick et al., 2000), which is sometimes accompanied by optic nerve atrophy (Jouet et al., 1994; Schrander-Stumpel et al., 1995). L1 knock-out mice display a number of these features, including axon guidance errors in the corticospinal tract and corpus callosum, cortical dendrite abnormalities, enlarged ventricles, hippocampal neuron loss, and eye defects with increasing age (Dahme et al., 1997; Cohen et al., 1998; Demyanenko et al., 1999). Interestingly, the L1 cytoplasmic domain contains a site for binding the cytoskeletal linker ankyrin B, whose knock-out in mice results in downregulation of L1 and subsequent degeneration of the optic nerve (Scotland et al., 1998).

To investigate a role for L1 in retinocollicular mapping, we traced the topographic projection of retinal axons to the SC in L1

Received April 8, 2002; revised Oct. 28, 2002; accepted Oct. 30, 2002.

This work was supported by National Institutes of Health Grants NS26620 and HD35170. We thank John Flanagan and David Feldheim for advice and reagents and Yoichiro Shibata and David Higgins for excellent technical assistance.

Correspondence should be addressed to Patricia F. Maness, Department of Biochemistry and Biophysics, CB7260, University of North Carolina School of Medicine, Chapel Hill, NC 27599-7260. E-mail: srclab@med.unc.edu.

 0270-6474/03/230530-09$15.00/0

null mutant mice by DiI labeling. Temporal axons of L1 mutant mice consistently displayed a bypass phenotype in which they overshot synaptic targets in the anterior SC and extended into the inferior colliculus (IC) or terminated inappropriately in the posterior SC. Mistargeting along the mediolateral axis of the SC also occurred but was more variable. The retinocollicular phenotype of L1-minus mice demonstrates that retinal axons require L1 in addition to EphA receptors to achieve topographic specificity of synaptic targeting.

Materials and Methods

Production and genotyping of L1 mutant mice. L1-minus mice used in this work were originally produced by homologous recombination in embryonic stem cells by Dr. Philippe Soriano (Fred Hutchinson Cancer Research Center) (Cohen et al., 1998). For our studies L1-minus mice on a 129/SvImJ congenic background were generated by mating heterozygous $L1^{-/+}$ females with wild type males (129/SvImJ) to yield hemizygous $L1^{-/y}$ males and wild-type male littermates, which were used as controls. RNA isolated from the brain of these L1 mutant mice contained no L1 transcripts detectable by reverse transcription-PCR (Fransen et al., 1998). Neither the full-length 200 kDa L1 protein nor shorter fragments were detected by immunoblotting (Cohen et al., 1998). No L1 immunoperoxidase staining was observed in the brain or retina of L1-minus mice. Genotypes of all mice were determined by PCR analysis as described previously (Demyanenko et al., 1999). A limiting factor in these studies was the reduced frequency of the L1-minus hemizygous male genotype produced in these matings (~10%), which deviated from the expected Mendelian frequency (25%) because of reduced viability and maternal care deficits.

Immunoperoxidase staining. Mouse embryos at embryonic day 18 (E18; day 18 gestational age) and postnatal day 0 (P0; day of birth) mice were killed by decapitation and fixed without perfusion in 4% paraformaldehyde in 0.1 M sodium phosphate buffer, pH 7.4. P10 and adult (86–170 d of age) mice were anesthetized with 20% urethane (0.1 ml/10 gm) and perfused transcardially with 4% paraformaldehyde in 0.1 M sodium phosphate buffer, pH 7.4. Brains and retinas were removed and stored at 4°C overnight in the same fixative, followed by storage for 2–3 d at 4°C in 30% sucrose and 0.13 M phosphate buffer. Frozen serial sections were cut at 10 or 20 μm in the coronal or horizontal orientation on a Minotome Plus microtome (Triangle Biomedical Sciences). The level of the section was indicated by Bregma distances from the interaural line as defined by Franklin and Paxinos (1997).

To visualize L1 expression, immunoperoxidase staining was performed using a mouse monoclonal antibody against the neural cell adhesion molecule L1 (L30220; Transduction Laboratories, Lexington, KY; 1:50). Sections were incubated with 0.1% H_2O_2, washed in PBS, blocked in 2% normal horse serum and 2% bovine serum albumin in PBS, and then incubated with primary antibody at 4°C overnight. Sections were washed and incubated with biotinylated anti-mouse IgG (Vector Laboratories, Burlingame, CA; 1:500 dilution) for 2 hr at room temperature. The remaining steps of immunocytochemistry were performed by the avidin–biotin–peroxidase method using a Vectastain kit according to the manufacturer's protocol (Vector Laboratories). Sections were counterstained with toluidine blue and photographed under bright-field illumination. The expression and distribution of ephrin-A2 were analyzed similarly by immunoperoxidase staining using an affinity-purified rabbit polyclonal antibody (20 μg/ml) against ephrin-A2 (L-20, sc-912) from Santa Cruz Biotechnology (Santa Cruz, CA). Ephrin-A ligands were detected by affinity probe *in situ* labeling in brain whole mounts using the receptor affinity probe EphA3 coupled to alkaline phosphatase (Cheng et al., 1995; Feldheim et al., 1998). The probes were gifts from Dr. John Flanagan (Harvard Medical School, Boston, MA).

Axonal tracing. L1-minus male mice and wild-type littermates were analyzed at P0 and P10–P14. Mice were anesthetized with AErrane (Baxter Health Care Corporation, McGaw Park, IL), and anterograde tracing of retinal axons was performed by focal injection of DiI (Molecular Probes, Eugene, OR) as a 10% solution in dimethylformamide into the extreme peripheral region of the temporal retina following the protocol of Simon and O'Leary (1992). Briefly, DiI was introduced by pressure injection with a Picospritzer II (General Valve, Fairfield, NJ) through a glass micropipette (tip internal diameter, ~50 μm), which was inserted into the periphery of the temporal retina near the dorsal-ventral midpoint through a small hole made in the sclera of the eye with a sharp tungsten needle. This hole served to orient the subsequent marking cuts. The injection site covered ~3–5% of the retina. After a survival period ranging from 24 to 72 hr, the mice were deeply anesthetized with 20% urethane and perfused transcardially with buffered 4% paraformaldehyde (PFA). Before removing the retina, 2 incisions were made around the injection site, and then 2 additional incisions were made, so that the 4 marking cuts demarcated the 4 quadrants of the retina. In some instances, DiI crystals were applied using the tip of a needle to the retina of mice that were perfused transcardially with buffered 4% PFA. These brains were stored at 37°C for several months to allow diffusion. Fixed brains were imbedded in 4% agar in an 11% sucrose solution and then sectioned horizontally at 200 μm using a vibratome. Axons labeled with dye were examined and photographed using a rhodamine filter for DiI. Alternatively, the superior and inferior colliculi, optic nerve with chiasm, as well as injected retinas were whole-mounted onto glass slides and examined under epifluorescence illumination. The boundaries of the SC and IC were determined from their characteristic shape and location. The injection sites of all retinas was verified by fluorescence imaging of flat mounts. There was no difference in size or location of retinal injections or general structure of the retina that could be responsible for the altered projections observed in L1-minus mice. Terminal arborizations were verified by their branched appearance at high magnification.

For whole eye fill experiments, we injected a 0.2% solution of cholera toxin β subunit labeled with fluorescein isothiocyanate into one eye and a 0.2% solution of cholera toxin β labeled with tetramethylrhodamine (List Biological, Campbell, CA) into the other eye of anesthetized wild-type and L1-minus mice at P10–P14. Solutions (2–5 μl in DMSO) were pressure-injected through a glass micropipette using the Picospritzer II. After 5 d, the mice were again anesthetized with 20% urethane (0.1 ml/10 gm) and perfused transcardially with 0.1 M PBS. Whole mounts of the midbrain were analyzed under epifluorescence illumination at sites contralateral to the injected eye using the appropriate rhodamine (for DiI) or fluorescein (for DiO) filters.

All images were captured with a Nikon microscope and Optronics TEC-470 CCD video camera system using an Apple Macintosh 840AV computer with a Scion LG-3 capture card (University of North Carolina Microscopy Services Laboratory; Dr. Robert Bagnell, director). Color overlay images were made using Adobe Photoshop and The Image Processing Tool kit (version 2.5; John Russ and Chris Russ, http://members.aol.com/ImagProcTK).

Results

L1 expression in the retinocollicular pathway

The expression of L1 in the developing retinocollicular pathway was analyzed by immunoperoxidase staining of sections from the retina and midbrain of wild-type mice. Most growth cones of RGC axons in the mouse migrate to the contralateral SC, where they grow over the SC surface in the superficial gray stratum and stratum opticum, overshoot their normal termination zones (TZs) by P0, and then branch and arborize in the region of the future TZ. Remodeling of the overshooting axon segment by P10–P15 results in a mature map (Flanagan and Vanderhaeghen, 1998; Frisen et al., 1998). At E18, when RGC axon growth to the SC was robust, L1 was expressed by neuronal cells in the ganglion cell layer (Fig. 1*A*). L1 expression appeared to be relatively uniform across the nasal-temporal axis of the retina. At P0, when many RGC axons were present over the SC surface, L1 continued to be expressed in RGC cells and their axons in the nerve fiber layer and appeared generally uniform across the nasal-temporal axis of the retina (Fig. 1*C*). L1 staining also appeared more or less uniform across the retinal dorsal-ventral axis at P0 (Fig. 1*E*). L1 immunoreactivity was also evident in the SC from E18 to P10, as

seen in horizontal sections near the SC surface (Fig. 1*F–H*) and in sagittal sections (Fig. 1*J–L*). L1 immunoreactivity was apparent in the superficial gray stratum and stratum opticum, sites that correspond to the location of incoming RGC axons (Fig. 1*I,K*). In the deeper layers of the SC, it was not possible to discriminate L1 expression on RGC axons from possible expression on collicular neurons. L1 immunoreactivity was less prominent in the IC than in the SC (Fig. 1*F,G,J,K*). Expression of L1 decreased substantially in the SC during maturation of the retinotopic map from P0 to P10 (Fig. 1*H,L*) and was barely detectable in the adult (Fig. 1*M*) as described previously (Bartsch et al., 1989; Lyckman et al., 2000). At each location and stage, staining for L1 was specific, and nonimmune IgG was negative (Fig. 1*B,D*, *insets*). Thus L1 was preferentially expressed on RGC axons during the period of axon growth and was downregulated with maturation.

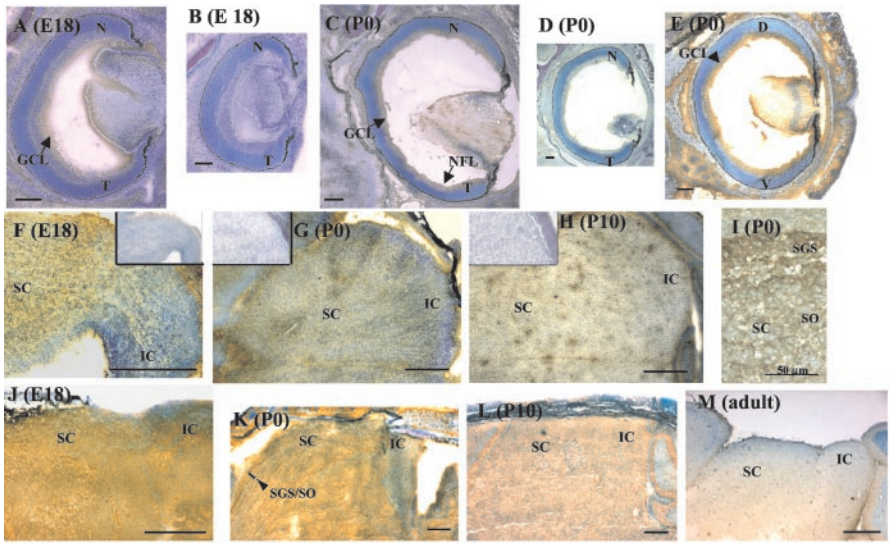

Figure 1. Expression of L1 in the developing retina and colliculi of wild-type mice. Immunoperoxidase staining for L1 in the retina of wild-type mice at E18 (*A, B*) and P0 (*C–E*) shows a relatively uniform distribution of L1 immunoreactivity in RGC bodies in the ganglion cell layer (*GCL*) and their axons in the nerve fiber layer (*NFL*) along the temporal (*T*)-nasal (*N*) axis and dorsal (*D*)-ventral (*V*) axis of the retina. *B, D*, Nonimmune Ig control staining. Immunoperoxidase staining for L1 in horizontal sections through superficial regions of the midbrain in wild-type mice at E18 (*F*) and P0 (*G*) shows L1 expression in the SC and lower levels in the IC. L1 immunoreactivity in the SC decreases by P10 (*H*). *Insets* show nonimmune Ig control staining. *I*, High magnification of SC at P0 showing L1 staining in the superficial gray stratum (*SGS*) and stratum opticum (*SO*). Sagittal sections of the same regions at E18 (*J*), P0 (*K*), P10 (*L*), and adult (*M*) show L1 immunoreactivity in the superficial gray stratum and stratum opticum (*SGS/SO*) and deeper in the SC both at E18 and P0, with lower levels in the IC. L1 staining decreased at P10 and adult stages. Scale bars: *A–E*, 100 μm; *F–H, J–M*, 500 μm; *I*, 50 μm.

L1 mutant mice display abnormalities in mapping of retinal axons

To test whether L1 was involved in the retinocollicular topographic mechanism, we mapped the projection of retinal axons to target sites in the SC of wild-type and homozygous L1 knockout mice by anterograde labeling with DiI. It has been established that (1) RGC axons from the far temporal retina of wild-type mice project to contralateral sites within the anterior SC, whereas RGC axons from the far nasal retina project to contralateral sites in the posterior SC; (2) RGCs of wild-type mice at intermediate locations along the temporal-nasal axis of the retina project to intermediate sites along the anteroposterior axis of the SC; and (3) the dorsal-ventral axis of the retina maps to the mediolateral axis of the SC (Simon and O'Leary, 1992; Frisen et al., 1998; Brown et al., 2000; Feldheim et al., 2000; Mui et al., 2002). In our study, DiI was introduced into the peripheral temporal retina of wild-type and L1-minus mice by focal injection or implantation of DiI crystals at P10–P14, when the retinocollicular map of the mouse is mature. Serial horizontal sections (200 μm) of the midbrain of wild-type and L1-minus mice were analyzed contralateral to the site of DiI labeling in the retina.

In P10–P14 wild-type mice. single retinal injections of DiI into the peripheral temporal retina near the dorsal-ventral midline gave rise to single DiI-labeled TZs in the anterior SC in all mice (19 of 19), as expected (Fig. 2*A,B*). High magnification of the anterior SC showed that labeled axons branched profusely at these sites forming terminal arbors (Fig. 2*A*, *inset*). The site of the TZ along the mediolateral axis of the anterior SC was more or less centrally located in all 19 cases. In striking contrast, DiI-labeled temporal retinal axons of L1-minus mice ($n = 10$) were observed at posterior locations within the SC or IC (Fig. 2*E,F,J,K,Q*). Labeled temporal axons of L1 mutant mice bypassed the proper termination site in the anterior SC in every case (10 of 10 mice). Often the DiI-labeled temporal axons of L1-minus mice (7 of 10) projected laterally to the posterior SC (Fig. 2*E,F,K*). Temporal axons were capable of forming TZs at these inappropriate posterior sites (Fig. 2*E,F*, *arrows*). However, some temporal axons could also be seen that continued in their trajectory to the IC (Fig. 2*E,F,J,K*). Within the IC, branching or arborization of temporal axons was never observed (Fig. 2*P*). In some L1-minus mice (3 of 10), DiI-labeled temporal axons were found in the posterior SC either in the central region (Fig. 2*J*) or near the midline border, where they formed multiple TZs (Fig. 2*Q*). The observed deviations were not attributable to variation in the sites of DiI injection, as shown by the relatively consistent labeling of retinas after whole mounting for each case (Fig. 2). Injection sizes of DiI varied to some degree, labeling ~3–5% of the retina. Dorsal injections of DiI at the nasal-temporal midpoint of wild-type mice gave rise to TZs that mapped to the lateral SC (data not shown), but errors of such magnitude were not produced by the peripheral temporal injections. There was no evidence for defasciculation or altered migration of temporal retinal axons toward the optic disk observed in flat mounts. The overall size and shape of the eye of L1 mutant mice and the presence of normal retinal architecture with all neuronal cells and plexiform layers properly oriented suggested that the absence of L1 did not affect retinal development or eye formation (R. Peiffer, G. P. Demyanenko, and P. F. Maness, unpublished results).

In summary, the most consistent feature of the L1-minus retinotopic map was a "bypass" phenotype in which temporal retinal axons overshot anterior targets and projected inappropriately to posterior sites in the SC or IC. Mistargeting along the mediolateral axis of the SC also occurred with a lateral bias but was variable.

To evaluate whether retinal axons filled the entire SC despite topographic mapping errors, a rhodamine- or fluorescein-labeled cholera toxin β subunit was injected into the eyes of wild-type and L1 mutant mice at P10–P14, when the retinotopic map was mature, to anterogradely label RGCs throughout the retina and to observe their contralateral projections. Analysis of whole mounts of five wild-type

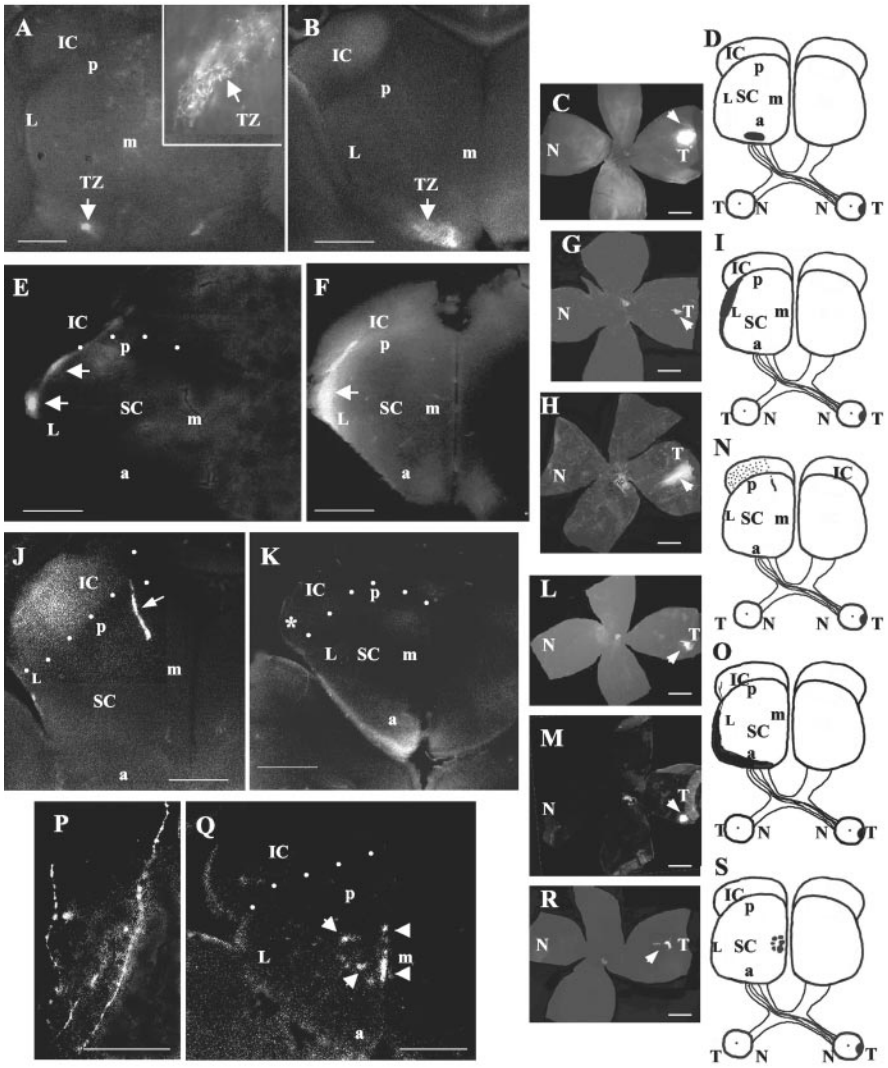

Figure 2. Mapping abnormalities of temporal retinal axons in L1-minus mice at P10. *A, B*, Horizontal sections (200 μm) from the SC of two wild-type mice labeled at P10 in the far temporal retina showing the single, centrally located DiI-labeled TZ in the anterior SC under epifluorescence illumination 48 hr after injection. *A, Inset*, High magnification of termination zone at the site of the *arrow* shown in *A*. *C*, Flat mount of wild-type P10 retina corresponding to the map in *B* 48 hr after injection visualized under epifluorescence illumination. *D*, Schematic illustration of retinocollicular projection of wild-type P10 mice shown in *A* and *B* based on analysis of serial sections. *E, F*, Horizontal sections from the SC of two different L1-minus mice at P10 showing DiI-labeled temporal axons at abnormal posterior-lateral sites in the SC (*arrows* indicate TZs). *J*, Horizontal section from the SC of an L1-minus mouse at P10 showing DiI-labeled temporal axons abnormally in the posterior SC extending close to the SC–IC border (*arrow*). Diffuse labeling of axons could be seen in the IC, but TZs were not observed. *K*, Horizontal section from the SC of an L1-minus mouse at P10 showing DiI-labeled temporal axons extending into the posterior SC and IC (*asterisks*) at the lateral edge. The labeled axons in the anterior SC did not form a terminal arbor. *P*, High magnification at the site of the *asterisk* in *K* showing unbranched L1-minus P10 temporal axons in the IC. *Q*, Horizontal section from the SC of an L1-minus mouse at P10 showing DiI-labeled temporal axons terminating in multiple TZs (*arrows*) at abnormal posterior sites within the central to medial region of the SC. *G, H, L, M, R*, Flat mounts of L1-minus retinas corresponding to maps in *E, F, J, K*, and *Q*, respectively, 48 hr after injection visualized under epifluorescence illumination. *I, N, O, S*, Schematic illustrations of retinocollicular projections of L1-minus P10 mice shown in *F, J, K*, and *Q*, respectively, based on analysis of serial sections. *a*, Anterior; *l*, lateral; *m*, medial; *N*, nasal; *p*, posterior; *T*, temporal. Scale bars: *A–C, E–H, J–M, Q, R*, 500 μm; *P*, 20 μm.

colliculi showed that contralateral projections of wild-type RGC axons filled the entire SC but did not label the IC (Fig. 3*A*). Whole mounts of four L1 mutant colliculi showed that contralateral projections of L1-minus RGC axons filled most of the SC with little labeling in the IC (Fig. 3*B*). In all L1 mutants, gaps were seen in the anterior SC that varied in their position among individuals and between hemispheres of the same animal, as shown in Figure 3*B*. The smaller gap near the center of both wild-type and mutant SC probably represented the injection site. At high magnification, some RGC axons of L1 mutant mice were seen to extend beyond the posterior border of the SC into the IC (Fig. 3*C*), but most axons were confined to the SC. In contrast-labeled axons of wild-type mice were not seen in the IC when observed by high magnification. These results suggested that most RGC axons of L1 mutant mice finally mapped to contralateral sites targeting the posterior SC and much of the anterior SC, whereas only a few axons were present in the IC. In the absence of L1, the mature retinotopic map appeared to have gaps in the anterior SC, perhaps because of insufficient remodeling of axons to occupy sites left vacant by posteriorly migrating temporal axons.

Branching of RGC axons during map development in L1 mutant mice

During development of the mouse retinocollicular projection, temporal wild-type RGC axons initially bypass their targets in the anterior SC at early postnatal stages (P0–P5) and extend into the posterior SC, with a few axons entering the IC (Frisen et al., 1998; Yates et al., 2001). Interstitial branches then form along the axon shaft and arborize within the region of the future TZ; subsequently, the overshooting axon is remodeled to form a mature map (Simon and O'Leary, 1992; Simon et al., 1994; Yates et al., 2001). To evaluate the ability of L1-minus RGC axons to branch and arborize during development, DiI injections were made in the peripheral temporal retina of L1-minus and wild-type mice at P0 to label temporal RGC axons, which show the greatest degree of overshoot (Yates et al., 2001). Temporal RGC axons of wild-type and L1-minus mice at P2 bypassed the anterior SC and extended into the posterior SC and IC as reported previously for wild-type mice (Fig. 4*A*). In horizontal sections (200 μm) of the SC and IC contralateral to the site of retinal DiI labeling, temporal axons of wild-type mice ($n = 3$) arborized in the anterior SC, the region of the future TZ (Fig. 4*B*). Wild-type temporal axons at P2 were also located in the posterior SC, and a few extended into the IC (Fig. 4*C*). In contrast, L1-minus temporal axons ($n = 3$) at P0 did not branch within the anterior SC (Fig. 4*D*,*E*) but arborized extensively in the posterior SC (Fig. 4*F*). Little interstitial branching was seen along the temporal axons of L1-minus mice at this stage anterior to the sites of arborization in the posterior SC. These results suggested that regulation of branching of temporal RGC axons in the vicinity of the future TZ in the anterior SC might be impaired during development in L1 mutant mice.

To evaluate whether ephrin-A expression was altered in L1-minus mice, immunoperoxidase staining for ephrin-A2 was performed on serial sections along the anteroposterior axis of the SC

in wild-type and L1-minus mice at P0. Ephrin-A2 is expressed normally in SC neurons of the mouse in a high posterior to low anterior gradient (Davenport et al., 1998; Feldheim et al., 2000). Neuronally expressed ephrin-A2 may be especially important in repelling temporal axons from posterior sites in the mouse, because mouse retinal axons avoid the most superficial layers of the SC, where ephrin-A5 is enriched (Davenport et al., 1998). Ephrin-A2 immunoreactivity was comparable for both wild-type and L1-minus SC and was distributed in a high posterior to low anterior gradient (Fig. 4*G–J*). In addition, labeling of the SC with an affinity probe consisting of the EphA3 receptor fused to alkaline phosphatase, which binds multiple ephrin-As, including ephrin-A2 and ephrin-A5 (Feldheim et al., 2000), revealed no differences in the midbrain of wild-type and L1-minus mice at P0 (data not shown).

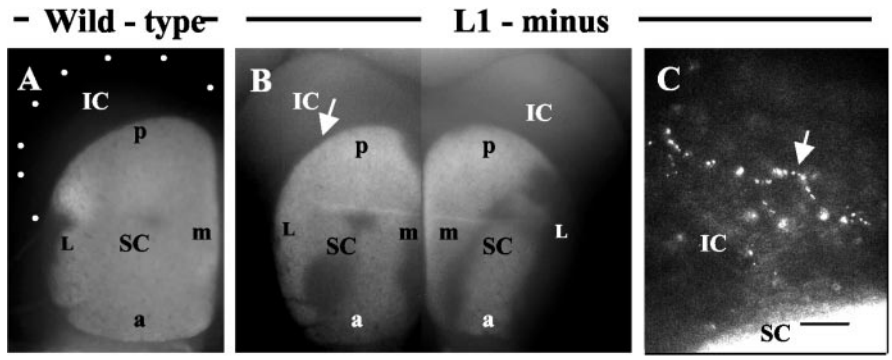

Figure 3. Retinal axons labeled with fluorescent cholera toxin β subunit by eye fill injection incompletely fill the superior colliculus of L1-minus mice. *A*, Retinal axons labeled with cholera toxin β fill the entire contralateral SC of wild-type mice at P12–P15. The posterior border of the IC is shown by the *dotted line*. *B*, Retinal axons labeled with cholera toxin β fill much of the contralateral SC of L1-minus-type mice labeled at P12–P15, with gaps in the anterior SC as shown in two hemispheres from the same mutant mouse separately labeled with fluoresceinated or rhodamine-labeled cholera toxin β and visualized individually using separate filters. *C*, High magnification of the regions indicated in *B* (*arrow*). *a*, Anterior; *l*, lateral; *m*, medial; *p*, posterior. Scale bar, 20 μm.

Normal midline crossing and fasciculation of the optic nerve in L1 mutant mice

The optic chiasm is an important midline decision point for sorting retinal ganglion axons that will project ipsilaterally or contralaterally as required for binocular vision. To evaluate whether L1-minus RGC axons might be impaired in their ability to select and enter the correct contralateral or ipsilateral optic tract in the absence of L1-expressing neurons at the optic chiasm, DiI crystals were placed onto the optic disk of one eye to label a maximum number of contralaterally and ipsilaterally projecting axons in L1-minus and wild-type mice at P10. In whole-mount preparations, most labeled RGCs in the optic nerve crossed the midline at the optic chiasm to the contralateral optic tract in both wild-type and L1 knock-out mice (Fig. 5*A,B*). L1-minus mice also showed a small ipsilateral projection like that of wild-type mice. The optic nerve and tract of L1-minus and wild-type mice also exhibited a similar degree of fasciculation at P10 (Fig. 5) and adult. Direct measurement of the diameter of the optic nerve of adult mice showed no significant differences in the means for wild-type (385 ± 8 μm; $n = 21$) and L1 mutant (392 ± 15 μm; $n = 4$) mice by the two-tailed t test ($p \leq 0.05$). The mean width of the optic chiasm measured at the midline was also not significantly different for wild-type (980 ± 88 μm; $n = 11$) and L1-minus (883 ± 109 μm; $n = 3$) mice. The mean width of the optic nerve measured 100 μm posterior to the midline was also the same for wild-type (880 ± 72 μm) and L1-minus (883 ± 109 μm) mice. Thus, in the absence of L1, RGC axons appear to fasciculate within the optic nerve and to cross the midline normally with a small ipsilateral projection.

Discussion

The findings reported here reveal a novel role for the cell adhesion molecule L1 in synaptic targeting of retinal axons. DiI labeling of L1-minus RGCs revealed an unexpected bypass phenotype in which temporal axons overshot anterior SC targets and projected inappropriately to posterior sites in the SC or IC. Mistargeting along the mediolateral SC axis also was evident, with a bias toward lateral sites. Despite the established ability of L1 to mediate axon growth and fasciculation, axons lacking L1 formed a fasciculated optic nerve with axons that crossed the optic chiasm and reached the SC; however, mutant axons from the temporal retina did not appear to arborize in appropriate anterior SC target regions. Results suggested that retinal axons require the L1 cell adhesion molecule in addition to EphA repellent axon guidance receptors for topographic mapping in the superior colliculus.

The retinotopic map of L1-minus mice differed from the map of ephrin-A2 and -A5 knock-out mice in several ways. As in ephrin-A2 and ephrin-A5 single mutants and ephrin-A2/A5 double mutants (Frisen et al., 1998; Feldheim et al., 2000), temporal axons in L1-minus mutants tended to project to abnormally posterior SC positions. However, L1-minus temporal axons rarely produced normal anterior arborizations, in contrast to ephrin-A2 and -A5 single mutants, and they did not often produce multiple arborizations along the anteroposterior axis that were consistently seen in ephrin-A2/A5 mutants. Thus axons lacking L1 may be more compromised than those of ephrin-A2 or -A5 mutants in generating TZs along this axis. Furthermore, unlike mutant ephrin-A2/A5 retinal axons, which more or less filled the SC when development of the retinotopic map was complete, anterior gaps remained in the final retinotopic map of L1-minus mice, suggesting that axons failing to form stable synaptic connections might be eliminated by cell death, or that other axons may not be able to occupy vacant sites left by errant temporal axons. Mapping of retinal axons to mediolateral SC targets was skewed in both L1 and ephrin-A2 and -A5 mutants (Feldheim et al., 2000). L1 mutant temporal axons displayed a range of mediolateral errors, with 7 of 10 cases located laterally and 3 of 10 cases located centrally or at the midline. In contrast, temporal axons of ephrin-A2/A5 double mutant mice were not targeted to any specific mediolateral position and occurred at a lower frequency (4 of 15 mice; Feldheim et al., 2000). Thus, L1, as well as ephrins-A2 and -A5, may contribute to mediolateral positioning of retinal axons. However, the homeodomain protein Vax2 appears to be more important in specifying this axis, because its deletion produces more consistently lateralized projections of temporal axons (Mui et al., 2002). It should be noted that mediolateral errors caused by L1 deficiency might be a secondary consequence of anteroposterior errors, because mediolateral coordinates are attained by axonal branching after anteroposterior positioning is established (Simon and O'Leary, 1992).

The normal size of the optic nerve and tract in L1 mutants sug-

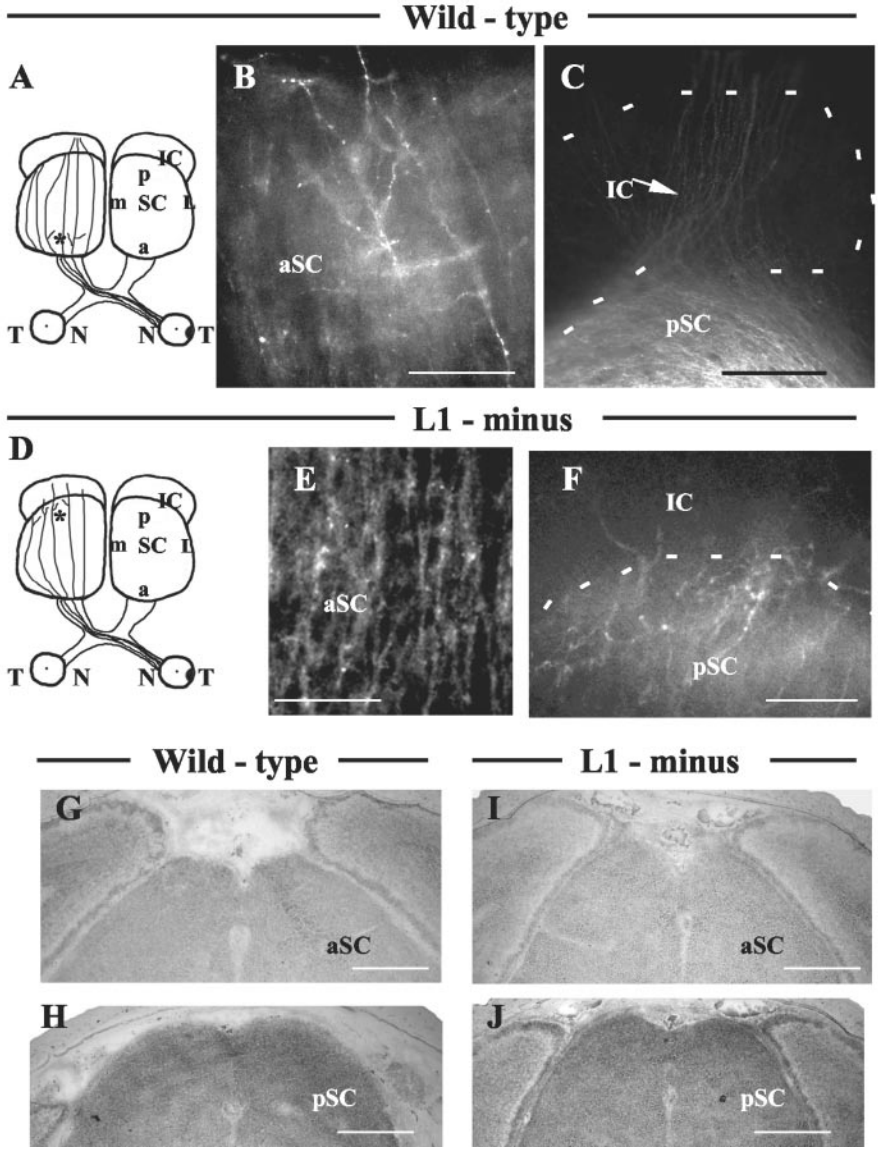

Figure 4. Branching of temporal retinal axons during map development in wild-type and L1-minus mice. *A*, Schematic illustration of the distribution of DiI-labeled temporal axons of wild-type mice at P2 bypassing future TZs in the anterior SC and extending over the entire SC with some axons present in the IC. *B*, DiI-labeled temporal retinal axons in wild-type P2 mice visualized by fluorescent microscopy of 200 μm horizontal sections showing branching in the region of the future termination zone in the anterior SC at the site indicated in *A* by the *asterisk*. C, DiI-labeled temporal retinal axons in wild-type P2 mice showing axons in the posterior SC and a few axons extending into the IC across the SC border. There was no evidence of axon branching in the posterior SC when observed at high magnification. *D*, Schematic illustration of the distribution of DiI-labeled temporal axons of L1-minus P2 mice. *E*, DiI-labeled temporal retinal axons in L1-minus P2 mice showing lack of branching in the anterior SC. *F*, DiI-labeled temporal retinal axons in L1-minus P2 mice showing axon branching in the posterior SC near the border with the IC at the site indicated in *D* by the *asterisk*. Immunoperoxidase staining of ephrin-A2 is shown in representative coronal sections through the SC of wild-type (*G*, *H*) and L1-minus (*I*, *J*) mice matched for location along the rostrocaudal axis. Ephrin-A2 immunoreactivity is similar in wild-type and L1 mutant mice, with little labeling in the anterior SC and strong labeling in the posterior SC. *a*, Anterior; *aSC*, anterior superior colliculus; *l*, lateral; *m*, medial; *N*, nasal; *p*, posterior; *pSC*, posterior superior colliculus; *T*, temporal. Scale bars: *B*, *C*, *E*, *F*, 20 μm; *G–J*, 500 μm.

gested that retinal axons exited the retina, crossed the midline, and entered the SC in appropriate numbers. Temporal axons of L1-minus mice appeared to be normally fasciculated within the retina as well as the optic nerve, but fasciculation of axons from other retinal locations was not analyzed. Antibody perturbation studies have shown that intraretinal axon fasciculation mediated by E587, a related member of the L1 family, is necessary to preserve the age-related order of RGC axons in the dorsal retina of the goldfish (Bastmeyer et al., 1995; Ott et al., 1998) and that axon fasciculation mediated by L1 can influence intraretinal axon guidance within the rodent retina (Brittis et al., 1995, 1996). Although L1 most likely contributes to RGC axon fasciculation, adhesive interactions of L1-related molecules such as neurofascin and NrCAM, which are also expressed in RGC axons (Bennett and Chen, 2001), might maintain fasciculation in the absence of L1.

The contribution of L1 to retinotopic mapping did not appear to arise from graded expression of L1 in the visual pathway. L1 was localized on RGC axons in the retina and superficial layers of the SC, in accord with previous studies (Lemmon and McLoon, 1986; Bartsch et al., 1989; Mi et al., 1998), but it was not expressed as a significant gradient across nasal-temporal or dorsal-ventral retinal axes. Eye enucleation experiments have confirmed that L1 within the SC is expressed primarily on RGC axons and not in underlying SC neurons (Lemmon and McLoon, 1986; Lyckman et al., 2000). Thus, retinotopic order is probably not specified by homophilic interactions between L1 on retinal axons and SC neurons but may be more likely mediated through heterophilic L1 interactions with ligands such as TAG-1, β1-integrins, F3/F11/contactin, and proteoglycans. Furthermore, the mapping abnormalities of L1 mutant axons did not appear to arise from altered ephrin-A expression, because the distribution and level of expression of ephrin-A2, and apparently other EphA ligands in the SC and IC of L1 mutants, were comparable with those of wild-type mice. L1 was clearly not essential for general RGC axon outgrowth, because L1 mutant axons extended from their positions within the retina through the optic tract to the SC in an apparently normal manner. Although RGC axon growth can be enhanced by cell adhesion molecules, it is primarily dependent on neurotrophins such as BDNF (Goldberg et al., 2002). Our results are in agreement with the initial development of an intact optic nerve in ankyrin B knock-out mice, in which L1 is downregulated (Scotland et al., 1998), and the long projection of corticospinal axons of L1 knock-out mice, in which midline crossing is perturbed (Dahme et al., 1997; Cohen et al., 1998). Although simple visual tests showed that L1-minus adult mice have a normal pupillary response to light and can see and track moving objects (P. F. Maness, W. Wetsel, and R. Rodriquez, unpublished observations), it is not known whether spatial acuity or functions of the superior colliculus were compromised.

As a precedent for correct targeting, it has been shown that temporal retinal axons initially overshoot their targets, form collateral branches within the region of the correct terminal posi-

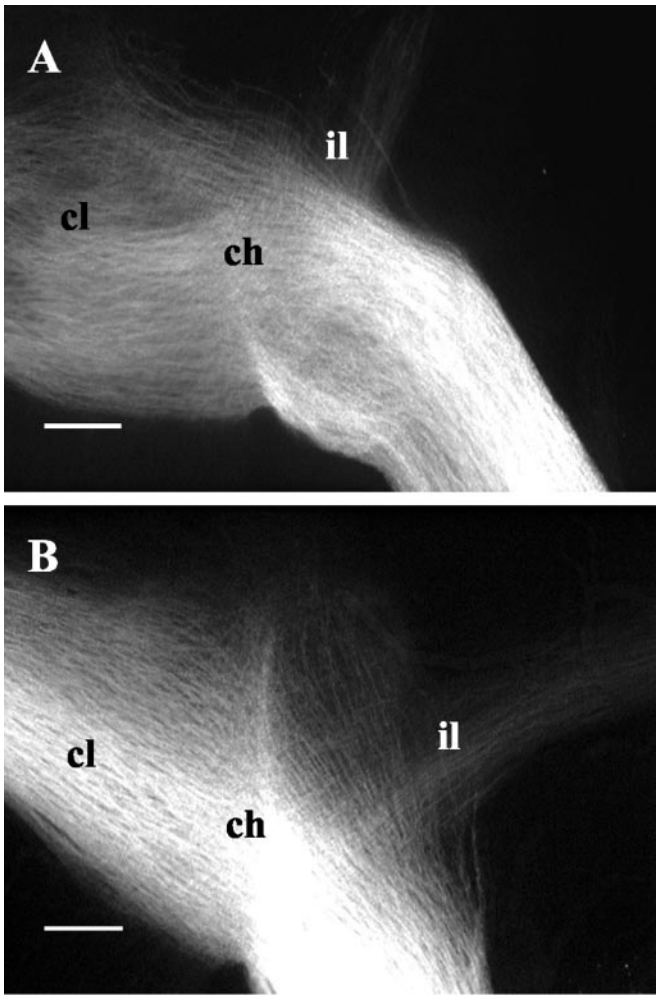

Figure 5. Retinal axons of L1-minus mice display normal crossing at the optic chiasm and fasciculation of the optic nerve. DiI-labeled axons in the optic nerve of wild-type (*A*) and L1-minus (*B*) mice are shown crossing at the optic chiasm (*ch*). Contralateral (*cl*) and ipsilateral (*il*) projections are of similar size in wild-type and L1 mutant mice. Scale bars, 100 μm.

tion, and then retract the overshooting axon segment (Simon and O'Leary, 1992). It has been suggested that ephrin- and EphA-induced branch suppression at incorrect positions posterior to the target zone is responsible for anterior targeting of temporal axons in the chick (Yates et al., 2001). At P2, both wild-type and L1-minus temporal axons extended across the anteroposterior axis of the SC, but mutant axons did not appear to form collaterals along the axon shaft in the anterior SC. A possible role for L1 in promoting axon branch formation topographically is supported by studies in transgenic mice in which ectopic expression of L1 on astrocytes alters the topographic organization of collateral branches of L1-positive corticospinal axons innervating the basilar pons (Ourednik et al., 2001). Other neural cell adhesion molecules can also regulate branch formation in retinal axons. Implantation of NCAM antibodies in the developing *Xenopus* tectum decreased terminal arbor branching and distorted the retinotectal map (Fraser et al., 1988), causing denuded areas of the tectum similar to the gaps in the eye fill map of L1 null mutants. N-cadherin antibodies also reduced branching of chick retinal neurons and altered the laminar distribution of their terminals in tectal slice overlay cultures (Inoue and Sanes, 1997). The inability of L1 antibodies to perturb axon branching in the latter study may have been attributable to loss of retinotopic information in their *in vitro* assays.

Adhesive interactions between L1 on retinal growth cones and homophilic or heterophilic ligands in the SC may serve to reduce the rate of axon growth, enabling rapid responses to repellent signals by ephrin-A2/A5. Indeed, the rate of axon growth by sensory neurons on L1 as a substrate is strikingly slower than on laminin (Liu et al., 2002). Alternatively, L1 could participate in retinotopic mapping by serving as a molecular switch for formation versus suppression of axonal branches. Formation of interstitial axon branches at correct targets may require dissociation of L1 from the actin cytoskeleton, leading to L1 clustering and activation of signaling through β1-integrins, c-Src, Rac1, and MAP kinase (Schmid et al., 2000). Consistent with this idea, Rac1 has an established role in stimulating neuronal process growth and branching (for review, see Luo, 2000), whereas integrins, Src, and MAP kinase promote neurite growth and migration (Schmid et al., 2000; Thelen et al., 2002). Reversible phosphorylation of a tyrosine residue in the cytoplasmic domain of L1 provides a mechanism by which L1 can be dissociated from the cytoskeleton and activated locally within the axon, because this modification negatively regulates the interaction of L1 family members with ankyrin and increases L1 lateral mobility within the membrane (Garver et al., 1997). Interestingly, the analogous Tyr-1229 of L1 is mutated to His in some L1 syndrome patients, abrogating ankyrin binding (Needham et al., 2001). Branch suppression within posterior segments of overshooting axons in wild-type mice could result from localized dephosphorylation of L1 at Tyr-1229, which would promote ankyrin recruitment and termination of L1 signaling. The posterior TZs found in some L1 knockout mice might be attributable to other attractant or trophic factors known to reside in the posterior SC (von Boxberg et al., 1993; Bahr and Wizenmann, 1996). Overshooting axon segments may fail to retract in L1 mutants because of lack of competition from interstitial axon branches, analogous to the process of atrophic retraction of terminal branches during synapse elimination at the developing neuromuscular junction (Keller-Peck et al., 2001).

Graded ephrin-A and EphA activation in the SC might oppose L1-induced axon growth or branching at the level of downstream intermediates of the L1 signaling pathway. For example, ephrin-A signaling through EphA receptors is capable of opposing neurite growth promoted by nonreceptor tyrosine kinases (Yu et al., 2001) and suppressing MAP kinase (Miao et al., 2001) and integrin function (Miao et al., 2000). Furthermore, ephrin-A and EphA signaling inhibits Rac1 and activates RhoA (Shamah et al., 2001), which is required for axon branch retraction (Billuart et al., 2001), RGC growth cone collapse (Wahl et al., 2000), and proper retinal axon targeting in *Xenopus* (Ruechhoeft et al., 1999). Alternatively, ephrin-A signaling might dephosphorylate L1 by recruiting tyrosine phosphatases to posterior axonal locations. In support of this notion, ephrin-A1 activation of EphA2 causes recruitment of the tyrosine phosphatase SHP2, dephosphorylating paxillin and focal adhesion kinase, resulting in decreased integrin-mediated adhesion (Miao et al., 2000).

References

Bahr M, Wizenmann A (1996) Retinal ganglion cell axons recognize specific guidance cues present in the deafferentated adult rat superior colliculus. J Neurosci 16:5106–5116.

Bartsch U, Kirchhoff F, Schachner M (1989) Immunohistological localization of the adhesion molecule L1, N-CAM, and MAG in the developing and adult optic nerve of mice. J Comp Neurol 284:452–462.

Bastmeyer M, Ott H, Leppert CA, Stuermer CAO (1995) Fish E587 glyco-

protein, a member of the L1 family of cell adhesion molecules, participates in axon fasciculation and the age-related order of ganglion cell axons in the goldfish retina. J Cell Biol 130:969–976.
Bennett V, Chen L (2001) Ankyrins and cellular targeting of diverse membrane proteins to physiological sites. Curr Opin Cell Biol 13:61–67.
Billuart P, Winter CG, Maresh A, Zhao X, Luo L (2001) Regulating axon branch stability: the role of p190RhoGAP in repressing a retraction signaling pathway. Cell 107:195–207.
Brittis PA, Lemmon V, Rutishauser U, Silver J (1995) Unique changes of ganglion cell growth cone behavior following cell adhesion molecule perturbations: a time-lapse study of the living retina. Mol Cell Neurosci 6:433–449.
Brittis PA, Silver J, Walsh FS, Doherty P (1996) Fibroblast growth factor receptor function is required for the orderly projection of ganglion cell axons in the developing mammalian retina. Mol Cell Neurosci 8:120–128.
Brown A, Yates PA, Burrola P, Ortuno D, Vaidya A, Jessell TM, Pfaff SL, O'Leary DD, Lemke G (2000) Topographic mapping from the retina to the midbrain is controlled by relative but not absolute levels of EphA receptor signaling. Cell 102:77–88.
Castellani V, Chedotal A, Schachner M, Faivre-Sarrailh C, Rougon G (2000) Analysis of the L1-deficient mouse phenotype reveals cross-talk between Sema3A and L1 signaling pathways in axonal guidance. Neuron 27:237–249.
Cheng HJ, Nakamoto M, Bergemann AD, Flanagan JG (1995) Complementary gradients in expression and binding of ELF-1 and Mek4 in development of the topographic retinotectal projection map. Cell 82:371–381.
Cohen NR, Taylor JS, Scott LB, Guillery RW, Soriano P, Furley AJ (1998) Errors in corticospinal axon guidance in mice lacking the neural cell adhesion molecule L1. Curr Biol 8:26–33.
Dahme M, Bartsch U, Martini R, Anliker B, Schachner M, Mantei N (1997) Disruption of the mouse L1 gene leads to malformations of the nervous system. Nat Genet 17:346–349.
Davenport RQQ, Thies E, Zhou R, Nelson PG (1998) Cellular localization of Ephrin-A2, Ephrin-A5, and other functional guidance cues underlies retinotopic development across species. J Neurosci 18:975–986.
Demyanenko GP, Tsai AY, Maness PF (1999) Abnormalities in neuronal process extension, hippocampal development, and the ventricular system of L1-knock-out mice. J Neurosci 19:4907–4920.
Feldheim DA, Vanderhaeghen P, Hansen MJ, Frisen J, Lu Q, Barbacid M, Flanagan JG (1998) Topographic guidance labels in a sensory projection to the forebrain. Neuron 21:1303–1313.
Feldheim DA, Kim YI, Bergemann AD, Frisen J, Barbacid M, Flanagan JG (2000) Genetic analysis of ephrin-A2 and ephrin-A5 shows their requirement in multiple aspects of retinocollicular mapping. Neuron 25:563–574.
Flanagan JG, Vanderhaeghen P (1998) The ephrins and Eph receptors in neural development. Annu Rev Neurosci 21:309–345.
Franklin KBJ, Paxinos G (1997) The mouse brain in stereotaxic coordinates. New York: Academic.
Fransen E, D'Hooge R, Van Camp G, Verhoye M, Sijbers J, Reyniers E, Soriano P, Kamiguchi H, Willemsen R, Koekkoek SK, De Zeeuw CI, De Deyn PP, Van der Linden A, Lemmon V, Kooy RF, Willems PJ (1998) L1 knockout mice show dilated ventricles, vermis hypoplasia and impaired exploration patterns. Hum Mol Genet 7:999–1009.
Fraser SE, Carhart MS, Murray BA, Chuong CM, Edelman GM (1988) Alterations in the *Xenopus* retinotectal projection by antibodies to *Xenopus* N-CAM. Dev Biol 129:217–230.
Frisen J, Yates PA, McLaughlin T, Friedman GC, O'Leary DD, Barbacid M (1998) Ephrin-A5 (AL-1/RAGS) is essential for proper retinal axon guidance and topographic mapping in the mammalian visual system. Neuron 20:235–243.
Garver TD, Ren Q, Tuvia S, Bennett V (1997) Tyrosine phosphorylation at a site highly conserved in the L1 family of cell adhesion molecules abolishes ankyrin binding and increases lateral mobility of neurofascin. J Cell Biol 137:703–714.
Goldberg JL, Espinoza JS, Xu Y, Davidson N, Kovacs GTA, Barres BA (2002) Retinal ganglion cells do not extend axons by default: promotion by neurotrophic signaling and electrical activity. Neuron 33:689–702.
Ignelzi Jr MA, Miller DR, Soriano P, Maness PF (1994) Impaired neurite outgrowth of src-minus cerebellar neurons on the cell adhesion molecule L1. Neuron 12:873–884.
Inoue A, Sanes JR (1997) Lamina-specific connectivity in the brain: regulation by N-cadherin, neurotrophins, and glycoconjugates. Science 276:1428–1431.
Jouet M, Rosenthal A, Armstrong G, MacFarlane J, Stevenson R, Paterson J, Metzenberg A, Ionasescu V, Temple K, Kenwrick S (1994) X-linked spastic paraplegia (SPG1), MASA syndrome and X-linked hydrocephalus result from mutations in the L1 gene. Nat Genet 7:402–407.
Keller-Peck CR, Walsh MK, Gan WB, Feng G, Sanes JR, Lichtman JW (2001) Asynchronous synapse elimination in neonatal motor units: studies using GFP transgenic mice. Neuron 31:381–394.
Kenwrick S, Watkins A, DeAngelis E (2000) Neural cell recognition molecule L1: relating biological complexity to human disease mutations. Hum Mol Genet 9:879–886.
Klein R (2001) Excitatory Eph receptors and adhesive ephrin ligands. Curr Opin Cell Biol 13:196–203.
Lemmon V, McLoon SC (1986) The appearance of an L1-like molecule in the chick primary visual pathway. J Neurosci 6:2987–2994.
Lemmon V, Farr KL, Lagenaur C (1989) L1-mediated axon outgrowth occurs via a homophilic binding mechanism. Neuron 2:1597–1603.
Liu R-Y, Schmid R-S, Snider WD, Maness PF (2002) NGF enhances sensory axon growth induced by laminin but not by the L1 cell adhesion molecule. Mol Cell Neurosci 20:2–12.
Luo L (2000) Rho GTPases in neuronal morphogenesis. Nat Rev Neurosci 1:173–180.
Lyckman AW, Moya KL, Confaloni A, Jhaveri S (2000) Early postnatal expression of L1 by retinal fibers in the optic tract and synaptic targets of the Syrian hamster. J Comp Neurol 423:40–51.
Mechtersheimer S, Gutwein P, Agmon-Levin N, Stoeck A, Oleszewski M, Riedle S, Fogel M, Lemmon V, Altevogt P (2001) Ectodomain shedding of L1 adhesion molecule promotes cell migration by autocrine binding to integrins. J Cell Biol 155:661–673.
Mi ZP, Weng W, Hankin MH, Narayanan V, Lagenaur CF (1998) Maturational changes in cell surface antigen expression in the mouse retina and optic pathway. Brain Res Dev Brain Res 106:145–154.
Miao H, Burnett E, Kinch M, Simon E, Wang B (2000) Activation of EphA2 kinase suppresses integrin function and causes focal adhesion kinase dephosphorylation. Nat Cell Biol 2:62–69.
Miao H, Wei BR, Peehl DM, Li Q, Alexandrou T, Schelling JR, Rhim JS, Sedor JR, Burnett E, Wang B (2001) Activation of EphA receptor tyrosine kinase inhibits the Ras/MAPK pathway. Nat Cell Biol 3:527–530.
Mui SH, Hindges R, O'Leary DDM, Lemke G, Bertuzzi S (2002) the homeodomain protein Vax2 patterns the dorsoventral and nasotemporal axes of the eye. Development 129:797–804.
Needham LK, Thelen K, Maness PF (2001) Cytoplasmic domain mutations of the L1 cell adhesion molecule reduce L1–ankyrin interactions. J Neurosci 21:1490–1500.
Ott H, Bastmeyer M, Stuermer CAO (1998) Neurolin, the goldfish homolog of DM-GRASP, is involved in retinal axon pathfinding to the optic disk. J Neurosci 18:3363–3372.
Ourednik J, Ourednik V, Bastmeyer M, Schachner M (2001) Ectopic expression of the neural cell adhesion molecule L1 in astrocytes leads to changes in the development of the corticospinal tract. Eur J Neurosci 14:1464–1474.
Ruechhoeft ML, Ohnuma S, McNeill L, Holt CE, Harris WA (1999) The neuronal architecture of *Xenopus* retinal ganglion cells is sculpted by rho-family GTPases *in vivo*. J Neurosci 19:8454–8463.
Schachner M (1991) Cell surface recognition and neuron-glia interactions. Ann NY Acad Sci 633:105–112.
Schaefer AW, Kamiguchi H, Wong EV, Beach CM, Landreth G, Lemmon V (1999) Activation of the MAPK signal cascade by the neural cell adhesion molecule L1 requires L1 internalization. J Biol Chem 274:37965–37973.
Schmid RS, Maness PF (2001) Cell recognition molecules and disorders of neurodevelopment. In: Handbook on brain and behavior in human development (Kalverboer AF, Gramsbergen A, eds), pp 199–218. Groningen, The Netherlands: Kluwer.
Schmid RS, Pruitt WM, Maness PF (2000) An MAPK signaling pathway mediates neurite outgrowth on L1 and requires Src-dependent endocytosis. J Neurosci 20:4177–4188.
Schrander-Stumpel C, Howeler C, Jones M, Sommer A, Stevens C, Tinschert S, Israel J, Fryns JP (1995) Spectrum of X-linked hydrocephalus (HSAS), MASA syndrome, and complicated spastic paraplegia (SPG1): clinical review with six additional families. Am J Med Genet 57:107–116.
Scotland P, Zhou D, Benveniste H, Bennett V (1998) Nervous system defects of ankyrin B (−/−) mice suggest functional overlap between the cell adhesion molecule L1 and 440-kD ankyrinB in premyelinated axons. J Cell Biol 143:1305–1315.

Shamah SM, Lin MZ, Goldberg JL, Estrach S, Sahin M, Hu L, Bazalakova M, Neve RL, Corfas G, Debant A, Greenberg ME (2001) EphA receptors regulate growth cone dynamics through the novel guanine nucleotide exchange factor ephexin. Cell 105:233–244.

Simon DK, O'Leary DD (1992) Development of topographic order in the mammalian retinocollicular projection. J Neurosci 12:1212–1232.

Simon DK, Roskies AL, O'Leary DD (1994) Plasticity in the development of topographic order in the mammalian retinocollicular projection. Dev Biol 162:384–393.

Thelen K, Kedar V, Paniker AK, Schmid RS, Midkiff BR, Maness PF (2002) The neural cell adhesion molecule L1 potentiates integrin-dependent cell migration to extracellular matrix proteins. J Neurosci 22:4918–4931.

von Boxberg Y, Diess S, Schwarz U (1993) Guidance and topographic stabilization of nasal chick retinal axons on target-derived components in vitro. Neuron 10:345–357.

Wahl S, Barth H, Ciossek T, Aktories K, Mueller BK (2000) Ephrin-A5 induces collapse of growth cones by activating Rho and Rho kinase. J Cell Biol 149:263–270.

Wilkinson DG (2001) Multiple roles of Eph receptors and ephrins in neural development. Nat Rev Neurosci 2:155–164.

Yates PA, Roskies AL, McLaughlin T, O'Leary DDM (2001) Topographic-specific axon branching controlled by Ephrin-As is the critical event in retinotectal map development. J Neurosci 21:8548–8563.

Yu H-H, Zisch AH, Dodelet VC, Pasquale EB (2001) Multiple signaling interactions of Abl and Arg kinases with the EphB2 receptor. Oncogene 20:3995–4006.

Zisch AH, Stallcup WB, Chong LD, Dahlin-Huppe K, Voshol J, Schachner M, Pasquale EB (1997) Tyrosine phosphorylation of L1 family adhesion molecules: implication of the Eph kinase Cek5. J Neurosci Res 47:655–665.